European Polymer Journal 239 (2025) 114255

Contents lists available at ScienceDirect

European Polymer Journal

journal homepage: www.elsevier.com/locate/europolj

One-pot non-isocyanate urethane synthesis via visible light-activated Curtius rearrangement

Vu Thi Tuyet Thuy [a], Saibal Jana [b], Wolfgang Wenzel [b], Patrick Theato [a,c], Azra Kocaarslan [b,d,*]

[a] Institute for Technical Chemistry and Polymer Chemistry (ITCP), Karlsruhe Institute of Technology, Engesserstraße 18, 76131 Karlsruhe, Germany
[b] Institute of Nanotechnology, Karlsruhe Institute of Technology (KIT) Hermann-von-Helmholtz Platz 1, 76344 Eggenstein-Leopoldshafen, Germany
[c] Institute for Biological Interfaces III (IBG-3) Soft Matter Synthesis Laboratory, Karlsruhe Institute of Technology (KIT), Hermann-von-Helmholtz-Platz 1, 76344 Eggenstein-Leopoldshafen, Germany
[d] Institute of Functional Interfaces (IFG) & Karlsruhe Institute of Technology (KIT), Hermann-von-Helmholtz-Platz 1, 76344 Eggenstein-Leopoldshafen, Germany

ARTICLE INFO

Keywords:
Isocyanate chemistry
Curtius rearrangement
light-induced Curtius rearrangement
Azide chemistry
Urethane chemistry

ABSTRACT

Curtius rearrangement is a highly versatile and powerful synthetic strategy for converting acyl azides into isocyanates. Herein, we introduce a visible-light-induced non-isocyanate method as an innovative ligation approach for urethane linkage formation, enabling the photochemical in situ generation of isocyanates under mild conditions. We design conjugated acyl azide molecules and successfully integrate these into diverse ligation processes, showcasing their versatility in small molecule synthesis, polymer chain-end functionalization, and surface modification of both inorganic and organic substrates. The resulting small molecules and materials were comprehensively characterized using nuclear magnetic resonance (NMR), attenuated total reflectance-Fourier transform infrared spectroscopy (ATR-FTIR), ultraviolet–visible (UV–Vis) and fluorescence spectroscopy, contact angle (CA) measurements, scanning electron microscopy (SEM), and transmission electron microscopy (TEM). Critically, density functional theory (DFT) calculations provided molecular-level insights into the reaction mechanism, revealing how electronic effects influence the initiation efficiency of acyl azides. Our simple yet highly efficient visible-light-driven ligation strategy paves the way for new applications in the fabrication of complex macromolecular architectures, advanced biomaterials, as well as hydrogel networks.

1. Introduction

Photochemical transformations performed at longer wavelengths (>350 nm) offer several key advantages, including enhanced penetration depth, reduced photodamage, and greater selectivity, making them particularly attractive for both material and biological applications [1,2]. These advantages have significantly propelled the development of visible- and near-infrared-light-mediated reactions over the past two decades, leading to notable progress in areas such as [2 + 2] photocycloadditions, photoisomerization, and photooxidation/reduction processes [3,4]. Despite these advances, the class of light-induced, self-driven organic rearrangement reactions—especially those that proceed without external reagents or catalysts—remains underexplored. These reactions represent a broad and vital class in which a molecule undergoes internal reorganization of its atomic connectivity, often resulting in the formation of C–O, C–N, and C–C bonds—key steps in natural product synthesis, drug development, and materials chemistry [5].

Among potential organic rearrangement reactions, the Curtius rearrangement (CR) —traditionally initiated by heat (~100) or UV-light (250 nm) exposure to convert acyl azides into isocyanates—emerges as a particularly promising target for visible-light activation [6,7]. Upon irradiation, acyl azides undergo a Curtius-type rearrangement to form isocyanates, accompanied by the release of nitrogen gas. The resulting isocyanates readily react with nucleophiles to yield the final products. Recent studies have further demonstrated that this rearrangement can also be induced by thermal treatment (60–70 °C) or by mechanical force, although these pathways differ mechanistically from the photochemical process [8–10]. This phosgene-free approach offers a safer and more sustainable route to synthesize isocyanate. Isocyanates (R–N=C=O or –

* Corresponding author at: Institute of Functional Interfaces and Institute of Nanotechnology, Karlsruhe Institute of Technology (KIT), Hermann-von-Helmholtz Platz 1, 76344 Eggenstein-Leopoldshafen, Germany.
E-mail address: azra.kocaarslan@kit.edu (A. Kocaarslan).

https://doi.org/10.1016/j.eurpolymj.2025.114255
Received 12 July 2025; Received in revised form 28 August 2025; Accepted 1 September 2025
Available online 2 September 2025

NCO) are indeed esters derived first from isocyanic acid, a highly unstable species synthesized by Wurtz in 1838 [11]. They are characterized by their pronounced reactivity toward nucleophiles, enabling their widespread use as intermediates in the synthesis of biologically active molecules (i.e., medicine, agrochemistry, and chemical biology) to advanced polymeric materials design (i.e., polyurethane and polyurea) [12–14]. Indeed, these highly reactive chemicals form the foundation of polyurethane and polyurea synthesis by reacting with polyols/polyamines in a fast and exothermic polyaddition reaction to generate urethane/urea linkages with or without the use of catalysts. The urethane linkage in the molecular structure offers many advantages, such as enhanced flexibility, abrasion, and chemical resistance, and so on [15–17].

Despite the urethane linkage providing quite an efficient final product, isocyanates are among the most widely criticized chemicals by climate activists and environmentalists due to the isocyanate-based synthesis and environmental concerns that lead to hazardous chemicals and long-term waste management problems [18–20]. In fact, isocyanate, upon inhaling, can severely and irrevocably affect the heart and lungs. Additionally, depending on pH, isocyanate produces unstable carbamic acid derivatives that promptly decarboxylate, resulting in primary amines. Unfortunately, this reactivity was tragically highlighted in 1984 when the uncontrolled reaction of methyl isocyanate with water led to one of the worst chemical industry disasters in Bhopal, India. Even after 40 years, the repercussions of this disaster remain evident, serving as a stark reminder of the catastrophic consequences of uncontrolled chemical reactivity [21]. In alignment with the growing emphasis on sustainable development and safer chemical design, research efforts have increasingly focused on developing milder, non-isocyanate synthetic routes [22]. Specifically, the CR emerges as a promising candidate for enabling non-isocyanate-based synthesis under light irradiation [23,24]. Thermal- and light-induced CR have been known for more than three decades,[25,26] light-induced variants have been insufficiently explored in synthetic methodology despite their potential advantages. While the thermal process requires close to 100 °C, non-substituted acyl azide compounds, particularly benzoyl azide, require invasive light irradiation (UV-C region, 254 nm).

This shorter wavelength requires high energy and strictly restricts the use of CR in biological applications. Previously, we have shown that CR is a versatile photo-ligation approach to obtain urethane linkage into the cross-linked polymer, onto the surface, and at the end of the polymer chain [27]. To address the limitations of harmful light exposure and harsh conditions, we hypothesize that a one-pot visible-light-driven Curtius rearrangement could provide a safer, more sustainable, and atom-economical route to urethane linkages. Our strategy focuses on rational molecular design to shift excitation wavelengths from the UV to the visible region by increasing the electron density of acyl azides, thereby enabling milder reaction conditions with enhanced selectivity and sustainability (Fig. 1A).

2. Results and discussion

It was a long-held principle in photochemistry that reactions perform optimally when irradiated at the wavelength of maximum absorption (λ_{max}). However, this principle also imposes several practical limitations in applications, including restricted light penetration depth, challenges in scaling photochemical processes for industrial use, reduced selectivity and control, and suboptimal energy efficiency [28]. To map photochemical reactivity, photochemical action plots (PAPs) provide a powerful tool for unravelling wavelength-dependent quantum yields, offering critical insights into how light energy dictates product distributions in photochemical reactions. Barner-Kowollik and coworkers have shown that by systematically correlating excitation wavelengths with reaction outcomes, action plot studies reveal complex wavelength-dependent reactivity and selectivity patterns that overturn conventional assumptions regarding the optimum irradiation wavelength in photochemical processes [29–32]. Therefore, we consider it essential to conduct preliminary studies aimed at addressing this aspect before

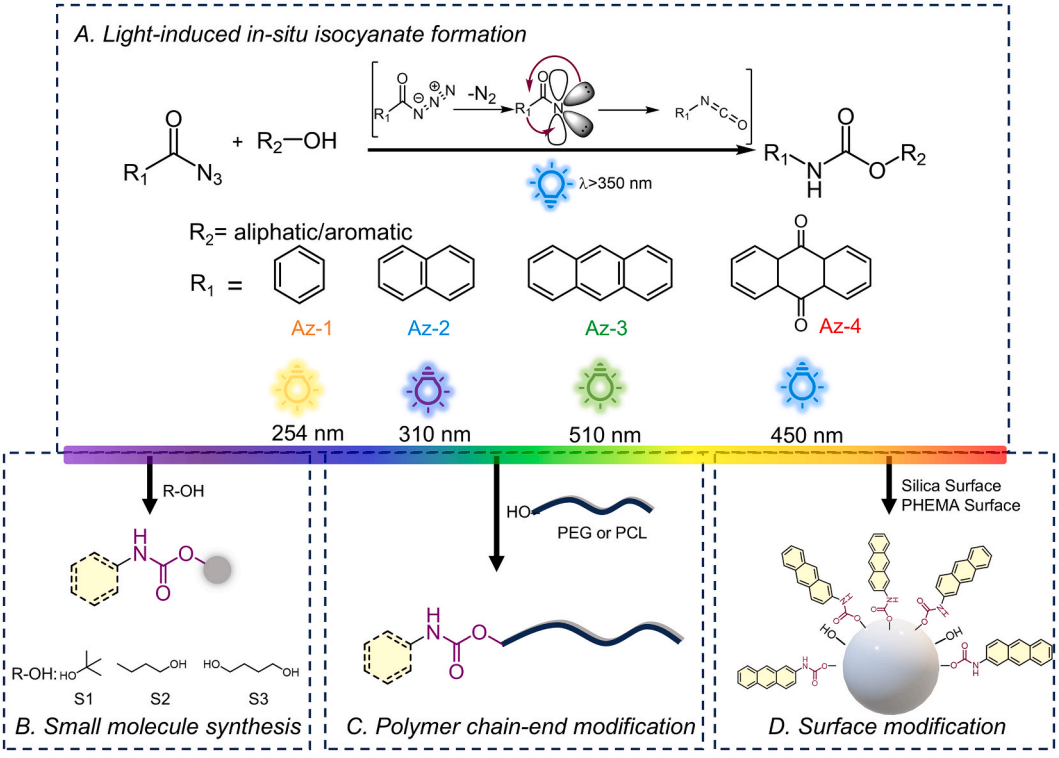

Fig. 1. A) The scheme represents the Curtius rearrangement (CR); acyl azide rearrangement to isocyanate moiety upon light irradiation. The filled ring demonstrated the aromatic structure of acyl azides. B) Small molecule synthesis via using CR reaction under light irradiation. C) Polymer chain-end modification via CR reaction under light irradiation. D) Silica surface modification via CR reaction under light irradiation.

performing light-driven experiments. It should be noted that action plot studies typically require precise light sources such as laser irradiation. As such laser sources were not available in our laboratory, we employed high-intensity fluorescence lamps and LEDs (λ_{max} is 250, 310, 365, and 410 nm) as alternative excitation sources. While this approach does not provide the same wavelength resolution as laser-based methods, it reliably demonstrates the photo-reactivity trends under irradiation and thus provides meaningful insights into the system's behavior. After identifying the optimal excitation wavelength, we systematically examined the solvent dependence of the reaction and utility of the visible light Curtius rearrangement across diverse applications. These included the synthesis of small organic molecules (Fig. 1B), the functionalization of polymeric materials (Fig. 1C), and the modification of surfaces (Fig. 1D). Expanding on our findings that the acyl azides can formally be activated by light irradiation (λ = 250 nm) through the elimination of the corresponding nitrogen ($-N_2$) release, we sought to investigate how the electron density on the acyl azide might impact the rearrangement of the carbon skeleton, which yields to isocyanate moiety.

We thus initiated our study by analyzing their photochemical reactivity of given aromatic acyl azides. Accordingly, different aromatic azides including benzoyl azide (**Az-1**), 2- naphthoyl azide (**Az-2**), 2-anthracene carbonyl azide (**Az-3**), and 2- anthraquinone carbonyl azide (**Az-4**) have been successfully synthesized from the respective acyl chlorides or carboxylic acids precursors, with full characterization given in the supporting information (Fig. S1-S4, S20-S29). Their electronic absorption properties were characterized by ultraviolet–visible (UV–Vis) spectroscopy (Fig. S5) to estimate the energy of their excited states and compare their reactivity under different irradiation energies varying from 250 nm to 510 nm. The $\pi \rightarrow \pi^*$ excited state of **Az-1** was recorded at a maximum absorbance of 250 nm, while **Az-2**, **Az-3**, and **Az-4** showed a red shift as expected. The $n \rightarrow \pi^*$ excited states of **Az-2**, **Az-3**, and **Az-4** were recorded at around 350 nm, 425 nm, and 330 nm, respectively. Additionally, fluorescence emission spectra were recorded for excitation at 360 nm, 450 nm, and 375 nm, respectively, which are rooted in the initial core structure (Fig. S6). The initial efforts were made to investigate CR under light irradiation at different wavelengths, including those corresponding to the maximum and minimum absorption of benzoyl azide, as well as wavelengths beyond its absorption range.

To investigate the rearrangement of **Az-1** into phenyl isocyanate, we followed the reaction in real-time by using FTIR spectroscopy in DCM at 250 nm, 310 nm, and 365 nm (Fig. 2- Fig. S45). A solution of Az-1 was prepared in a Schlenk tube, thoroughly deoxygenated by argon purging, and subsequently sealed with a specialized cap to allow in situ FT-IR probe measurements. Real-time FTIR analysis allows straightforward monitoring of the reaction through the disappearance of the characteristic azide peak at around 2100 cm^{-1} (real-time FTIR reaction set-up can be found in Fig. S44). Since the transformation from the acyl azide to the corresponding isocyanate was closely monitored, no nucleophilic species were added to the reaction medium.

The reactions as aforimentioned were carried out under a deoxygenated atmosphere in dry DCM at ambient temperature, and monitored until the azide peak had completely disappeared, indicating quantitative (or near-quantitative) conversion to the isocyanate. Real-time FTIR measurements of **Az-1** upon excitation at 254 nm and 310 nm are shown in Fig. 2A and 2B, capturing the progression of the reaction over time. The azide ($-N_3$) peak at 2136 cm^{-1} decreased dramatically, while isocyanate stretching vibration at 2260 cm^{-1} gradually increased, with irradiation at 254 nm giving the fastest formation of the isocyanate peak among the three different light irradiation conditions for **Az-1**. The C=O and C-N stretches, which correspond to acyl azide, were recorded at 1695 cm^{-1} and 1184 cm^{-1}, respectively, and were observed to decrease over time under 250 nm and 310 nm irradiation. The vibrations between 1593 cm^{-1} and 1417 cm^{-1}, attributed to the C=C stretches of the ring, remained unchanged, except for vibrations at 1593 cm^{-1} and 1511 cm^{-1}, which were assigned to N–H bending and C-N stretches. These results are consistent with literature findings [33]. For instance, Bornemann et al. reported that the photolysis of benzoyl azide at 254 nm and 308 nm predominantly yields phenyl isocyanate, with phenyl cyanate as a minor product. While irradiation with 254 nm and 310 nm can trigger molecular rearrangement, 365 nm showed no considerable isocyanate formation (Fig. S7A-C).

Similar to **Az-1**, the rearrangement of **Az-2** to isocyanate was observed under $n \rightarrow \pi^*$ state irradiation at 310 nm and 365 nm (Fig. 3). The characteristic isocyanate stretch at around 2266 cm^{-1} was formed under both irradiation wavelengths at 310 nm and 365 nm, no isocyanate formation was observed at 450 nm (Fig. S45). **Az-1** and **Az-2** have shown photo CR at both $n \rightarrow \pi^*$ and $\pi \rightarrow \pi^*$ excited states [34]. Different from Az-1 and **Az-2**, **Az-4** has shown no rearrangement to isocyanate at

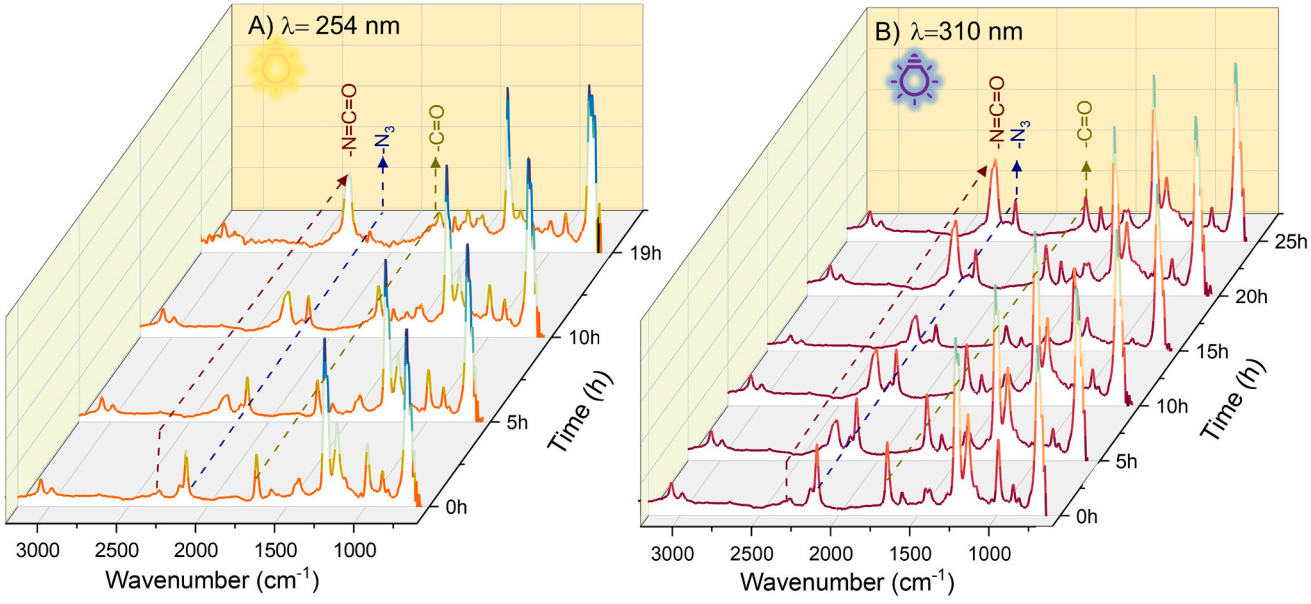

Fig. 2. Real-time FTIR monitoring of the light-induced Curtius rearrangement of benzoyl azide (Az-1) to phenyl isocyanate in DCM at ambient temperature under (A) 254 nm and (B) 310 nm irradiation.

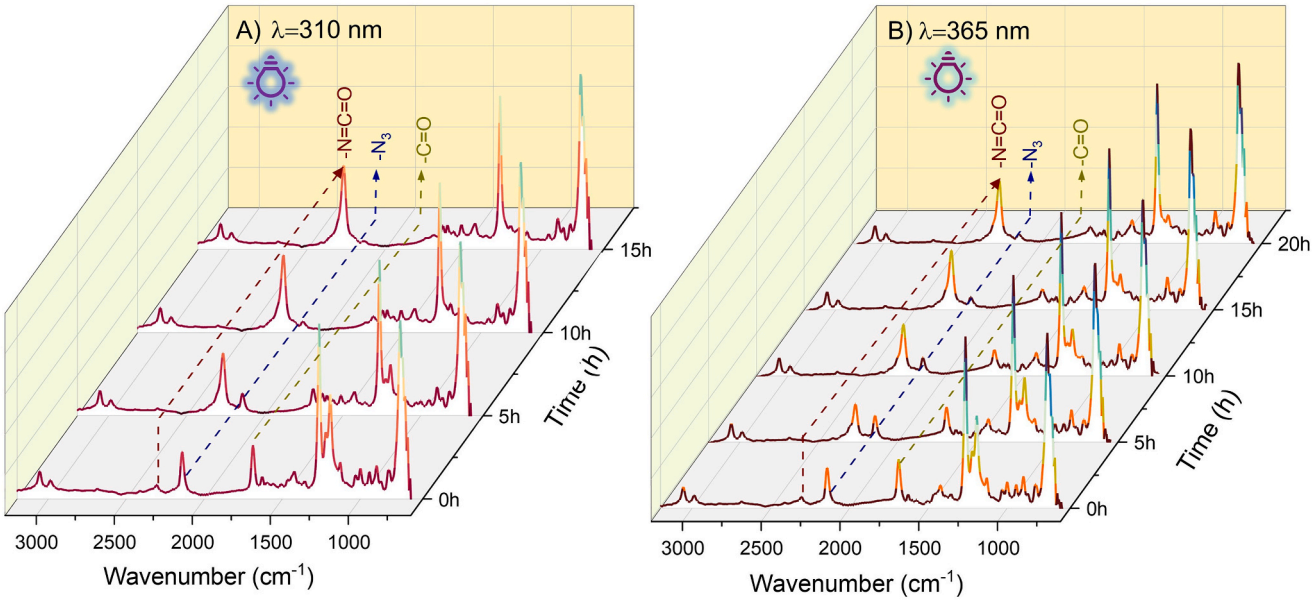

Fig. 3. Real-time FTIR monitoring of the light-induced Curtius rearrangement of benzoyl azide (Az-2) to isocyanate derivative in DCM at ambient temperature under (A) 310 nm and (B) 365 nm irradiation.

their n → π* transition energy of 365 nm, while **Az-3** produced unwanted products at both its π → π* transition energy of 310 nm and n → π* transition energy of 450 nm. Instead, **Az-3** showed its activation energy lower than its n → π* excited state energy at 510 nm.

2.1. *Photochemical Perspective and theoretical calculations*

According to previous femtosecond time-resolved studies in CR, the reaction follows a step-wise path and forms a nitrene intermediate together with isocyanate through the excitation states of acyl azides [35]. However, the exact mechanism of CR by photochemistry is still debated. For aroyl azides, Sigman *et al.* reported that rearrangement only occurs at π → π* excited states, while the n → π* state produces only nitrene [36]. However, Kubicki and his team claimed that both π → π* and n → π* singlet excited states of **Az-2** yield isocyanate and that nitrene is formed independently from these excited states, rather than serving as a precursor for isocyanate [37]. In contrast, Wentrup *et al.* suggested that for acyl azides, nitrene acts as an intermediate in isocyanate formation at both π → π* and n → π* singlet excited states, supported by FTIR and MS analysis [33]. To summarize, determining the exact mechanism of the photo-CR remains challenging. This reaction can proceed directly from the singlet excited state of acyl azides or through the excited states of nitrene, though side reactions involving nitrene can interfere.

To further solidify our understanding, molecular modelling and simulations can help us to provide explanations about experimentally observed reaction pathways. Previous computational studies for chlorodifluoroacetyl azide and isopropyl azides, given that nitrene is the intermediate of organic azides, overcome barrierless of 5 kJ·mol^{-1} and 1 kJ·mol^{-1} to form amine isomer and isocyanate, respectively [38,39]. However, computational studies have not yet been carried out on the proposed acyl azide derivatives under longer-wavelength irradiation. Therefore, to gain a deeper understanding of the photolytic CR on proposed acyl azide derivatives, we performed computational calculations using density functional theory (DFT) and time-dependent DFT (TD-DFT) methods. In this study, we systematically report the reaction pathways for the photoinduced CR of molecules **Az-1** through **Az-4** (Fig. S9-11). Upon irradiation with an appropriate wavelength of light, each molecule is excited to its singlet excited state via an electronic transition from the HOMO to the LUMO.

In this excited state, molecular nitrogen (N_2) readily dissociates from the azide through a low-energy transition state, generating a stable singlet intermediate (–CON). Subsequently, a rearrangement occurs, yielding the isocyanate (–NCO). Under photolytic conditions, the rearrangement step is typically rate-determining; however, when compared to the ground state geometry without light irradiation, the energy barrier for the initial N_2 elimination becomes the dominant factor. Consequently, the wavelength of the incident light plays a crucial role in initiating the CR, and its selection is solely dependent on the electron density of the molecules. Highly electron-dense systems require irradiation with longer wavelengths, whereas less electron-dense azides demand shorter wavelengths. Therefore, it is essential to illuminate the system with the appropriate wavelength to trigger the CR.

To further elucidate the mechanism, we computed the activation barrier heights for the two key transition states in each molecule:

Transition State 1 (N_2 elimination):

- For **Az-1**, **Az-2**, and **Az-3**, the N_2 elimination occurs via a barrier-less transition.
- For **Az-4**, the computed activation barrier is 8.4 kcal·mol^{-1}. Notably, **Az-4** requires relatively higher energy input for N_2 elimination compared to its counterparts, suggesting that its electronic structure facilitates the formation of a triplet state from the excited singlet state, allowing it to pass through the N_2 elimination transition state with less than 0.6 kcal·mol^{-1} of additional energy.

Transition State 2 (rearrangement to isocyanate):

- The activation barriers for the rearrangement step are 14.6 kcal·mol^{-1} for **Az-1** and 8.4 kcal·mol^{-1} for **Az-2**, whereas **Az-3** exhibits a barrierless transition, reflecting an ease of rearrangement for isocyanate formation.
- For **Az-4**, both singlet and triplet pathways are available for the rearrangement step. The singlet pathway is more favorable, requiring only 2.8 kcal·mol^{-1}, while the triplet pathway exhibits a higher computed barrier of 23 kcal·mol^{-1}. In **Az-4**, two competing reaction pathways create a trade-off. The singlet state is less efficient at eliminating N_2, but it makes up for this with an easier rearrangement step. On the other hand, the triplet state requires less energy for N_2 elimination but is less favourable when it comes to rearrangement.

Fig. 4 shows the excitation of Az-1 in the presence of 1-butanol under 287 nm irradiation. For Az-1, shorter-wavelength (higher-energy) light is required to trigger electronic excitation and initiate the reaction. In the presence of 1-butanol, the resulting isocyanate undergoes further reaction to yield the corresponding product via urethane linkage formation. Notably, this process proceeds through nearly identical activation barriers for all investigated azides (Fig. 4A). As the electron density on the aromatic rings increases via conjugation (observed in Az-2 and Az-3), the required irradiation shifts to longer wavelengths due to a significant reduction in the HOMO-LUMO gap (see Fig. 4B).

The choice of solvent is also critical in CR reaction—it must be inert to nitrene yet capable of facilitating the rearrangement. Kubicki and coworkers investigated the formation of isocyanate, nitrene, and triplet states in **Az-2** by employing IR and UV–Vis transient absorption spectroscopy after 350 nm excitation in halogenated solvents [37,40]. They have found that increasing solvent polarity raises the rate of isocyanate formation while reducing triplet and nitrene formation. Clauss *et al.* further supported this by proposing a mechanism where DCM insertion into nitrene facilitates rearrangement without additional photon energy [40]. They also demonstrated that agents like hydroxyl, carbonyl, electron-rich olefins, and fullerene C_{60} promote nitrene adduct formation. Peng and co-workers observed that carbonyl azides exhibit different excited-state lifetimes depending on the solvent polarity. Polar solvents such as methanol and acetonitrile stabilize excited carbonyl azides, resulting in relatively longer lifetimes and shifts in absorption maxima compared to non-polar solvents like cyclohexane. The relation between solvent polarity and the electronic states of the azides thus determines the kinetics of the photochemical reactions and the pathways of the product formation, illustrating the critical influence of solvent on reaction dynamics [35]. It should be noted that acetonitrile and dimethyl sulfoxide cause side reactions with nitrene intermediate. Therefore, we strategically investigate Az- 3 rearrangement reaction in two different solvents, namely, n-hexane, and DCM. Our solvent comparison indicates that DCM is the preferred medium for the CR of these molecules, as it facilitates a lower-energy reaction pathway (Fig. 5).

After taken into account computational and experimental studies we conducted, it can be proposed that DCM has potentially catalyzed the CR thermally as a Lewis acid via the electron-withdrawing effect; it weakens the C=O and the N=N adjacent while strengthening the C-N bond, resulting in a reduction of activation energy of the reaction and accelerating the reaction rate. While DMSO is predominantly basic and stabilizes azides, even in their excited states, no CR or nitrene formation occurs. We therefore continue to investigate the rearrangement of the other aromatic azides in DCM. When we investigated the kinetics of the photo CR in deuterated DCM, we also found that the rearrangement of aromatic azides has first-order kinetic and is nonlinear (Fig. S8).

In summary, this study reinforces previous findings that the CR of acyl azides can proceed via both $\pi \rightarrow \pi$ and $n \rightarrow \pi^*$ singlet excited states, or exclusively through the $\pi \rightarrow \pi^*$ state, depending on the acyl azide structure. Increasing electron density markedly lowers the activation barriers, thereby enabling visible-light-induced CR. For Az-4, both singlet and triplet pathways are accessible; however, the overall energy profile favors the triplet pathway due to its lower energetic demand, despite the singlet state providing a lower barrier for the rearrangement step. Computational results therefore support our hypothesis that longer-wavelength light can promote CR in electronically rich acyl azide derivatives. While preliminary action plot studies revealed an absorption–reactivity mismatch, a detailed wavelength-resolved analysis is currently underway to better understand this phenomenon. Elucidating the underlying mechanism will be the subject of a dedicated future study; here, we focus primarily on exploring the practical application scope of CR reactions with basic mechanistic insight.

CR reaction was further tested in the presence of different alcohol moieties under visible light irradiation. The **Az-4** has shown a different reaction pattern compared to the other acyl azides. Upon exposure to 365 nm light (n- π^* singlet excited states), **Az-4** did not rearrange into the isocyanate. However, surprisingly, we found out that the addition of alcohol initiated and accelerated the CR of **Az-4** at 450 nm in DCM while it did not happen in the light-deficient condition (Fig. S15). We hypothesized that the presence of hydroxyl groups has lowered the energy barrier. Therefore, subjecting the system to 450 nm light is sufficient for the CR to occur with significant yield (89 %), achieving 99 % conversion and eliminating nitrene formation (Fig. S34-S5).

We then conducted several reactions with **Az-3** as an acyl azide source, using different nucleophiles, namely butanol, *tert*-butanol, and butanediol, under irradiation at 510 nm. The same phenomenon occurred with **Az-3**, we observed a much faster rate of CR conversion in the presence of hydroxyl agents, leading to the formation of urethane linkages with 99 % conversion, high yields around 85 % without catalysts (Fig. 6). This important observation—that the presence of a hydroxyl agent accelerates urethane linkage formation—unlocks significant potential for the application of photo-induced CR in materials science, which has not previously been explored.

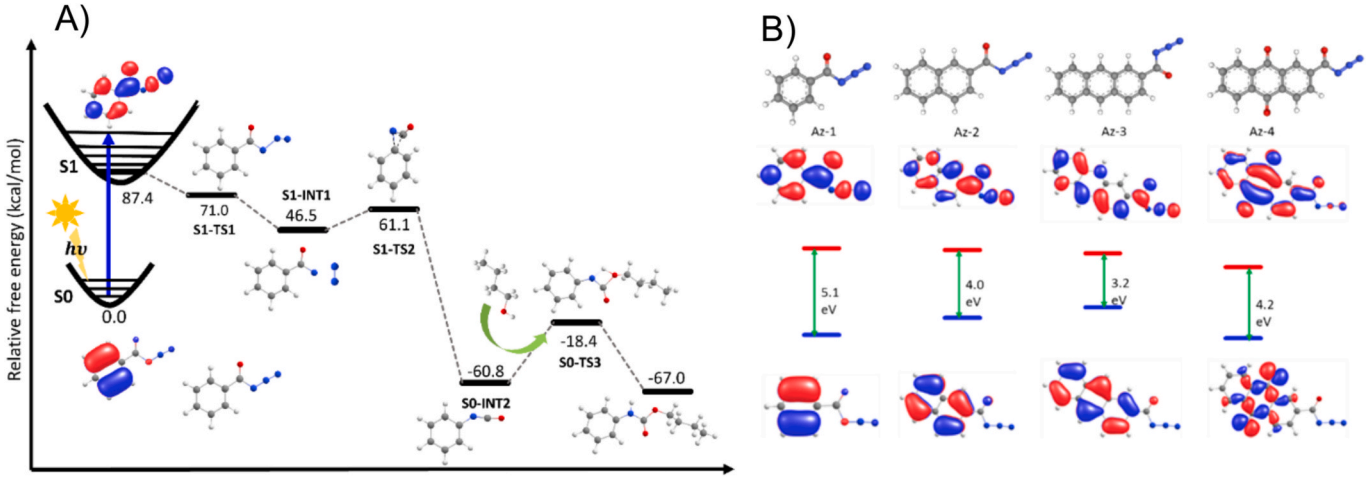

Fig. 4. A) Reaction energy profile for the Curtius rearrangement (CR) and functionalization of Az-1 in the presence of butanol. Here, energies are given in kcal·mol^{-1} and the incident photon has a wavelength of 287 nm. S0 and S1 denote the ground state and the excited singlet state, respectively; TS represents a transition state, and INT represents an intermediate, each labeled with its corresponding number. B) The highest occupied molecular orbitals (HOMO) and lowest unoccupied molecular orbitals (LUMO) of acyl azide derivatives from Az-1 to Az-4. The corresponding HOMO–LUMO energy gap is presented in electron volts (eV).

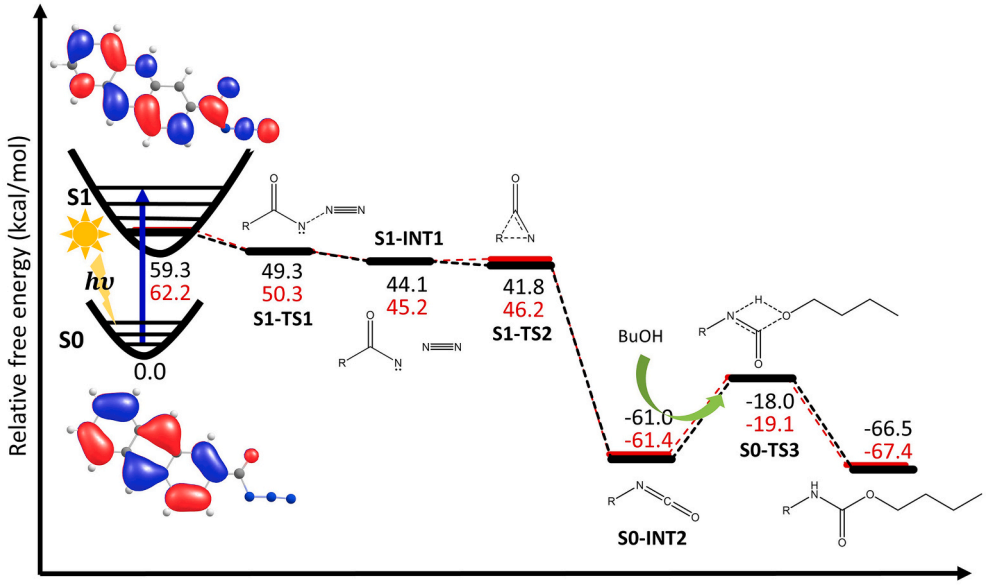

Fig. 5. Reaction energy profile for the Curtius rearrangement and functionalization of Az3 in the presence of BuOH. Energies are reported in kcal·mol^{-1}. An implicit solvation model was employed with two solvents –DCM and n-hexane- to evaluate solvation effects. Data from calculations in DCM are represented by black curves and numerical annotations, while those in hexane are depicted with red curves and numbers. S0 and S1 denote the ground and excited singlet states, respectively; TS indicates a transition state, and INT represents an intermediate, each identified by its corresponding number.

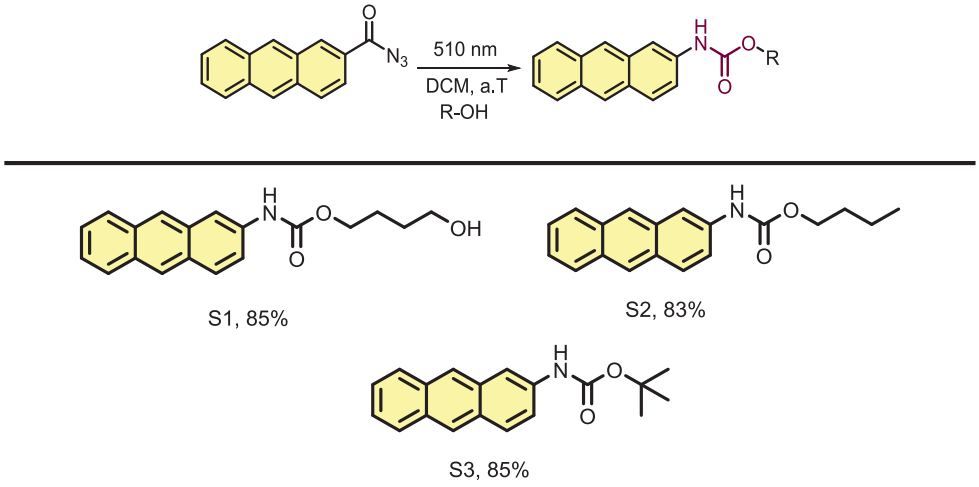

Fig. 6. Urethane linkage formation via light-induced Curtius rearrangement between Az-3 and different alcohol sources. The reaction conditions were as follows: Az-3 (1 eq.) and respective alcohol (20 eq.) were reacted under an inert atmosphere at ambient temperature in DCM. The reaction time = 24 h, λ = 510 nm. Conversions were calculated from ^{1}H NMR.

2.2. *Curtius rearrangement (CR) in applications*

Organic reactions can be applied in polymer chemistry to introduce new functionalities, expanding the scope of polymer modifications. These functionalization strategies have been widely utilized in designing telechelic polymers, surface modifications, grafting approaches, and bioconjugation. To demonstrate its capability in polymer modification, CR was further evaluated for chain-end functionalization of hydroxy-terminated polymers by reacting to the –hydroxyl groups of poly (ε-caprolactone) (PCL) and poly (ethylene glycol) (PEG) with Az-2 and Az-3 under 365 nm and 510 nm light irradiation, respectively (Fig. 7).

Size-exclusion chromatography (SEC) has shown a slight increase in molecular weight without a dramatic impact on dispersity (Fig. 7B) . It should be noted that, based on the SEC measurement (Fig. 7B), the reaction was completed without side-chain reactions or anthracene dimerization. The overall data associated with the photoinduced chain-end functionalization with Az-3 is represented in Table 1. Further ^{1}H NMR (Fig. S17) and FT-IR analysis of the functionalized PCL and PEG confirm the success of the chain-end modification process. In Fig. S17, the aromatic peaks appeared around 7.5–8.5 ppm, indicating the incorporation of an aromatic ring at the polymer chain ends, along with the characteristic proton of the urethane at ~ 10 ppm. Respective FTIR spectra of P1-P3 confirm the success of the chain-end modification process (Fig. 7C). The modified polymer spectra show that the –OH stretching peak at around 3450 cm^{-1} was disappeared and a new broader peak was observed at a lower wavenumber around 3300 cm^{-1}, which can be attributed to the –NH stretching vibration of the urethane linkage, together with CH sp^{2} stretching of the rings. Furthermore, –C=O stretching of the urethane linkage appeared at around 1730 cm^{-1} in the case of PEG modification, while in the case of PCL modification, –C=O stretching peaks overlapped with the PCL carbonyl group. For all chain-end modifications, the ring's skeleton vibrations appeared on

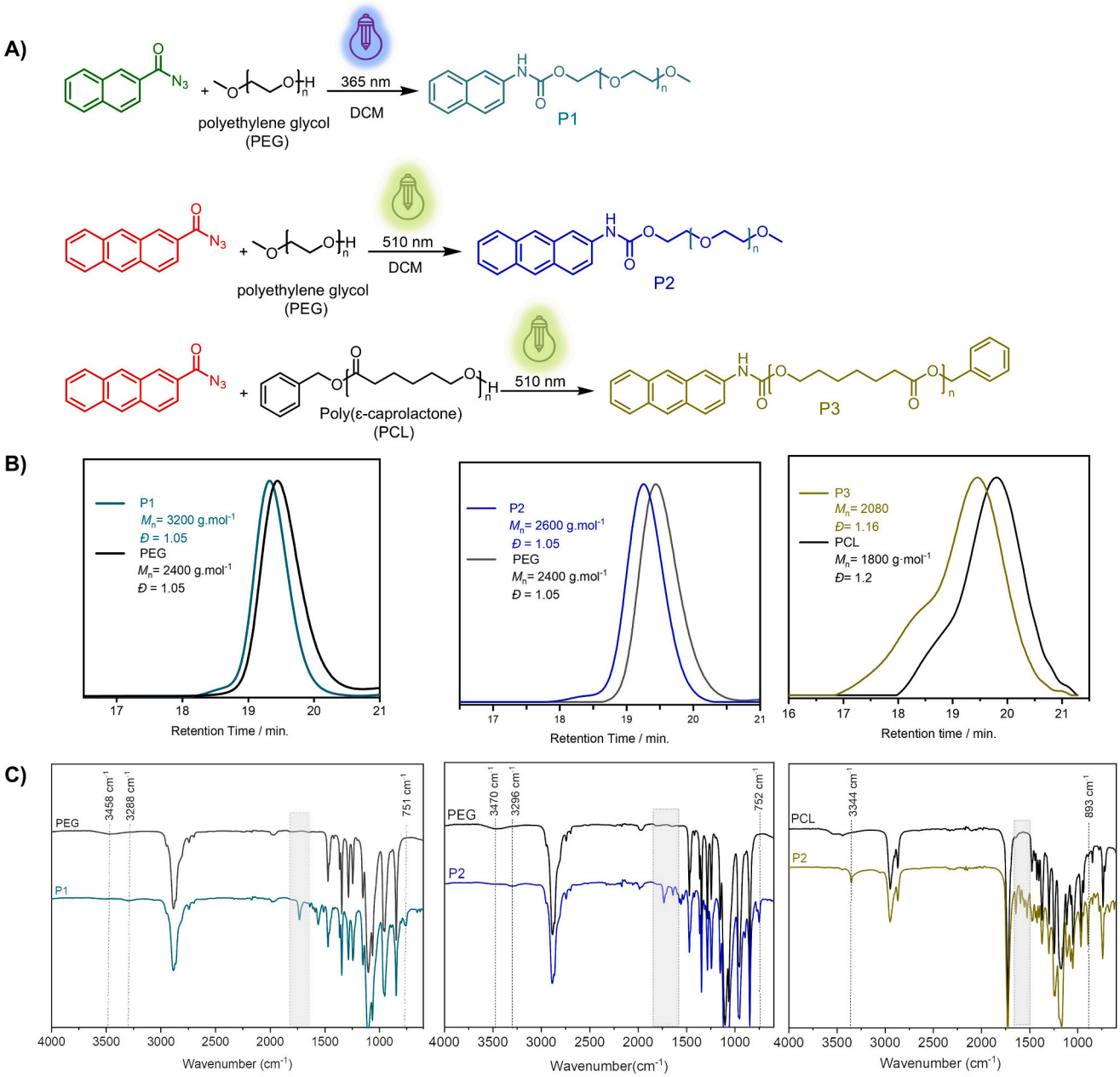

Fig. 7. A) Synthetic scheme of light induced chain end modification of PEG and PCL with Az-2 and Az-3. B) Comparative SEC traces PEG and PCL (black) P1 (green), P2 (blue) and P3 (dark yellow) C) FTIR spectra of PEG and PCL (black), P1 (green), P2 (blue) and P3 (dark yellow).

Table 1
Chain-end functionalization of polymers by light-induced urethane linkage formation[a].

Run	Isocyanate Source	Polymer structure	Yield[b] (%)	Đ
P2	Az-3	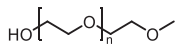	75	1.06
P3	Az-3	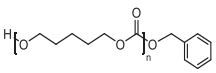	65	1.16

[a]Typical reaction conditions were as follows: Az-3 (1 eq.) and polymer (5 eq.) were reacted under an inert atmosphere at ambient temperature in DCM. The reaction time is 24 h, λ = 510 nm.
[b]The yield was calculated via gravimetric analysis.

1646 cm^{-1}, indicating the successful preservation of polymer backbone. The yields of the processes were found to be 75 % and 65 %, for PEG and PCL modification, respectively (Table 1).

These data demonstrate that CR can be used as an advantageous ligation approach for tailor-made chain-end design under mild conditions with non-invasive light sources. The obtained polymer has similar absorption characteristics to pure anthracene (Fig. S18A). The fluorescence spectrum of a diluted solution of anthracene-modified PEG and PCL in DCM excited at $\lambda_{ex.} = 360$ nm, showed the characteristic emission band of the excited (singlet) anthracene at 432 nm (Fig. S18B). These further observations clearly confirmed the successful chain-end functionalization.

Anthracene and naphthalene are valuable chemical structures known for their distinctive fluorescence under visible light. In addition to their photoluminescent properties, they exhibit well-characterized photo reactivity, undergoing dimensional reactions at 310 nm and

365 nm, respectively. That feature makes these molecules good candidates for forming photochemically driven reversible dynamic bonds in macromolecular structures [41]. In our investigation, we tested anthracene excimer formation with the anthracene chain-.modified PEG (Figure (A), which showed an excimer reaction at 365 nm, proven by the doubling of the molecular weight with SEC measurement (Fig. 8B and Table S1-S3). These results demonstrate strong potential for the formation of block copolymers from two distinct polymers, which synthesized via different methodologies, by using simple photochemical reactions under visible light.

Moreover, we aim to extend the scope of visible light induced Curtius rearrangement on surface modification. Inorganic material surface modification is a highly attractive research field to achieve desired characteristics in the materials, such as improved adhesion, corrosion resistance, catalytic activity, biocompatibility, or hydrophobicity. This process is widely used in material science, nanotechnology, and various industrial applications to enhance performance, durability, or interaction with target materials [42,43]. However, homogenous modification of the surface with a defined concentration and good accessibility of the immobilized components has been a key challenge that drastically affects the physicochemical properties of the materials obtained. Here, we proposed a new non-invasive light-induced ligation approach for the synthesis of composites with high homogeneity. To further extend the application of our profound strategy in polymer modification to surface modification, silica (Si-OH) surfaces (Fig. 1D-Fig. 9A) and PHEMA surfaces (Fig. 10) were functionalized with anthracene. Fig. 9A shows the comparison of bare and modified silica surfaces SEM images which indicates surface disturbance in the modified silica surface.

The representative TEM image of the resulting surface functionalization (Fig. 9B) confirms the successful ligation of the anthracene unit to the surface via a urethane linkage. Additionally, the high-angle annular dark-field scanning TEM (HAADF-STEM) image, along with the corresponding EDS mapping (Fig. 9C), reveals the nearly homogeneous dispersion of C and O atoms on the silica surface. Notably, the surface modification is also visible under 365 nm light irradiation. The characteristic fluorescent feature of anthracene is transferred to the silica surface (Fig. 9D).

Similarly, the poly (hydroxy ethyl methacrylate) (PHEMA) surface was successfully modified with anthracene through urethane linkages at 510 nm, resulting in a more hydrophobic surface with a 40° increase in water contact angle, reaching 110° compared to the pristine surface's 62° (Fig. 10). FT-IR result show urethane linkage formation with the slight change at 3340 and 1630 cm^{-1} (Fig. S19).

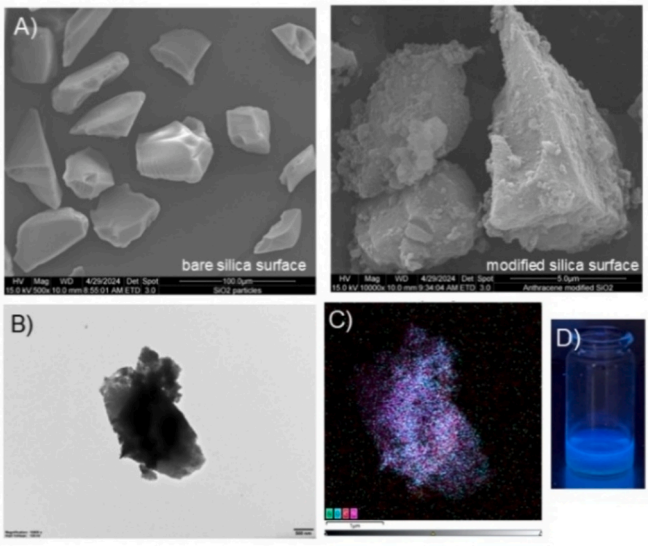

Fig. 9. A) SEM image of the modified silica surface. B) The high-magnification TEM image of the modified silica surface. C) HAADF-STEM image associated EDS elemental mapping for C, N, O, and Si atoms of the modified silica surface. D) The photograph of fluorescent emission of modified silica.

3. Conclusion

We herein report a photoinduced ligation strategy with broad applicability, encompassing synthesis, post-synthetic modification, and surface engineering. For the first time, we applied real-time FTIR analysis for light-induced reaction acyl azide rearrangements, enabling direct observation of the azide moiety in the reaction medium while the reaction progresses. The DFT calculations provided critical molecular-level insights into the reaction pathway, confirming the energetic feasibility of the photoinduced rearrangement and revealing the influence of electronic density on activation energy barriers. Out experimental studies have shown that polar solvent, particularly DCM can act as a catalyst in the system to support the rearrangement reactions. The urethane bond plays a crucial role in small molecules, surfaces, and macromolecules; therefore, we sought to emphasize the applicability of our proposed method through various demonstrations.

Our approach enables precise material functionalization upon visible-light exposure (510 nm), as demonstrated by the tailored physical properties of modified PHEMA through contact angle measurements

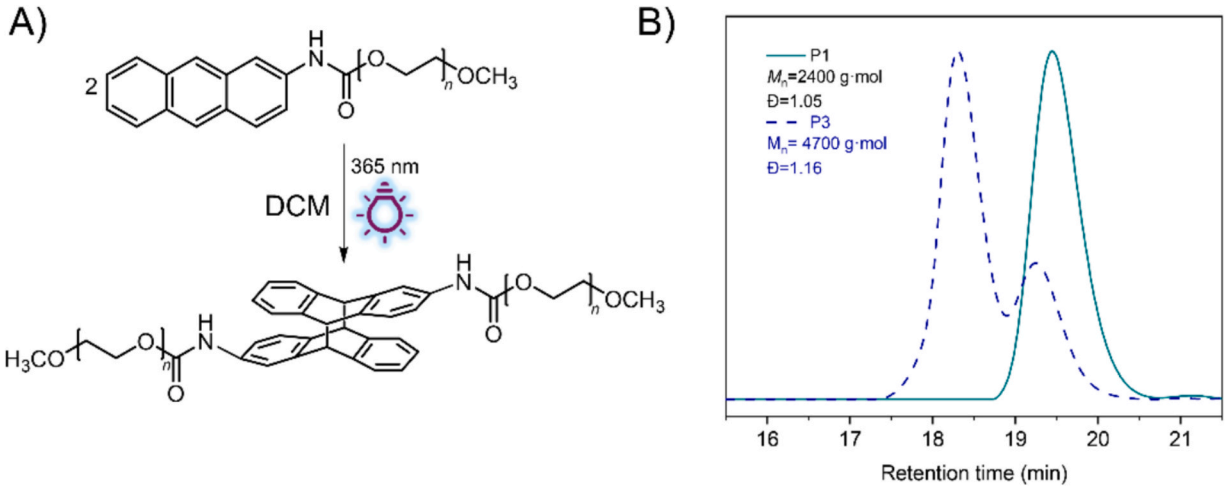

Fig. 8. A) Schematic representation of excimer formation between anthracene chain-end modified PEG polymers under 365 nm light irradiation. B) Comparative SEC traces P2 (green line) and P4 (blue dotted line) before and after excimer formation.

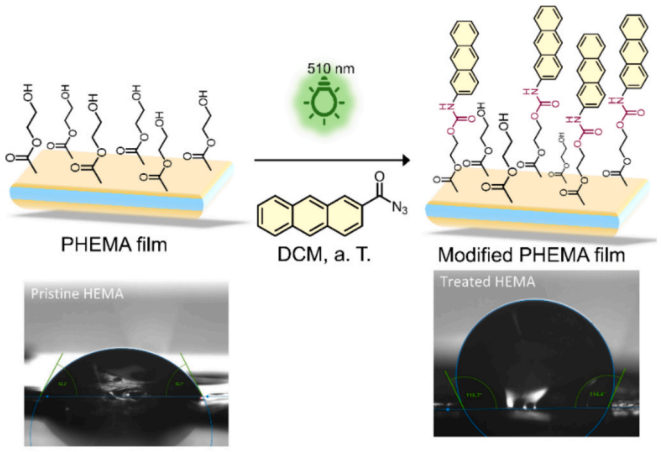

Fig. 10. Surface modification of PHEMA film and their side views for the drop at pristine and treated PHEMA surface.

and the formation of uniform silica coatings validated by SEM and TEM analyses. Elemental mapping further confirmed the incorporation of nitrogen and carbon, reinforcing the effectiveness of this method. Most importantly, this strategy facilitates on-demand isocyanate generation under mild and non-invasive conditions. In addition to the proposed study, precision photochemistry based on Curtius rearrangement continues to be explored. By employing hydroxyl- and other nucleophile-bearing precursors, this work paves the way for innovative material design through urethane linkage formation enabled by precise photochemistry.

Author contributions

The experimental studies were completed, and the first draft of the manuscript was prepared by V.T.T.T. The theoretical calculations were completed by S. J., and the calculation studies supervised by W. W. P. T. and A.K provided support during the project and manuscript preparation. This project was conceptualized and supervised by A.K.

CRediT authorship contribution statement

Vu Thi Tuyet Thuy: Investigation, Formal analysis, Data curation, Writing first draft. **Saibal Jana:** Visualization, Software, Investigation. **Wolfgang Wenzel:** Supervision. **Patrick Theato:** Writing – review & editing. **Azra Kocaarslan:** Writing – review & editing, Visualization, Supervision, Funding acquisition.

Declaration of competing interest

The authors declare that they have no known competing financial interests or personal relationships that could have appeared to influence the work reported in this paper.

Appendix A. Supplementary material

The supporting information includes materials, instrumentation experimental details and characterization of all synthesized compounds with $^{1}H/^{13}C$ NMR, ATR-FTIR and EIS-MS, fluorescence emission spectra of the acyl azides, modified polymers, real-time FTIR of Az-1 in different solvents (DMSO, DCM and n-Hxn), UV–VIS spectra of anthracene modified PEG and PCL, kinetic study of Az-3, anthracene modified PHEMA surface characteristics with contact angle measurements [44].

Supplementary data to this article can be found online at https://doi.org/10.1016/j.eurpolymj.2025.114255.

Data availability

Data will be made available on request.

References

[1] R.C. Evans, P. Douglas, H.D. Burrow, *Applied photochemistry*, Springer, 2013.
[2] M.S.N. Weerasinghe, T. Nwoko, D. Konkolewicz, Polymers and light: a love–hate relationship, Chem. Sci. 16 (2025) 5326.
[3] K. Kalayci, H. Frisch, V.X. Truong, C. Barner-Kowollik, Green light triggered [2+ 2] cycloaddition of halochromic styrylquinoxaline—controlling photoreactivity by pH, Nat. Commun.s 11 (2020) 4193.
[4] Q. Liu, B.B. Zhang, H. Sheng, S. Qiao, Z.X. Wang, X.Y. Chen, Visible-Light-induced photoreduction of carborane phosphonium salts: efficient synthesis of carborane-oxindole-pharmaceutical hybrids, Angew. Chem. 135 (2023) e202305088.
[5] S.K. De, *Applied Organic Chemistry: Reaction Mechanisms and Experimental Procedures in Medicinal Chemistry*, John Wiley & Sons, 2020.
[6] S. Shi, C. Yao, J. Cen, L. Li, G. Liu, J. Hu, S. Liu, High-fidelity end-functionalization of poly (ethylene glycol) using stable and potent carbamate linkages, Angew. Chem. Int. Ed. 59 (2020) 18172.
[7] G. Gody, C. Rossner, J. Moraes, P. Vana, T. Maschmeyer, S.B. Perrier, One-pot RAFT/"click" chemistry via isocyanates: efficient synthesis of α-end-functionalized polymers, J. Am. Chem. Soc. 134 (2012) 12596.
[8] L. Marinescu, J. Thinggaard, I.B. Thomsen, M. Bols, Radical azidonation of aldehydes, J. Org. Chem. 68 (2003) 9453.
[9] H. Lebel, O. Leogane, Boc-protected amines via a mild and efficient one-pot Curtius rearrangement, Organic Lett. 7 (2005) 4107.
[10] K. Yoo, E.J. Hong, T.Q. Huynh, B.-S. Kim, J.G. Kim, Mechanochemical regulation of unstable acyl azide: Ir (III)-catalyzed nitrene transfer C–H amidation under solvent-free ball milling conditions *ACS Sustainable Chem*, Eng 9 (2021) 8679.
[11] J. Wisniak, Charles-Adolphe Wurtz Educación Química 16 (2005) 347.
[12] S. Ozaki, Recent advances in isocyanate chemistry, Chem. l Rev. 72 (1972) 457.
[13] E. Vitaku, D.T. Smith, J.T. Njardarson, Analysis of the structural diversity, substitution patterns, and frequency of nitrogen heterocycles among US FDA approved pharmaceuticals: miniperspective, J. Med. Chem. 57 (2014) 10257.
[14] A.K. Ghosh, A. Sarkar, M. Brindisi, The Curtius rearrangement: mechanistic insight and recent applications in natural product syntheses, Org. Biomol. Chem. 16 (2018) 2006.
[15] J.O. Akindoyo, M.H. Beg, S. Ghazali, M.R. Islam, N. Jeyaratnam, A. Yuvaraj, Polyurethane types, synthesis and applications–a review, RSC Adv. 6 (2016) 114453.
[16] J.R. Ghonia, N.G. Savani, V. Prajapati, B.Z. Dholakiya, A review on polyurethane based multifunctional materials synthesis for advancement in textile coating applications, J. Polym. Res. 31 (2024) 95.
[17] M. Cui, Z. Chai, Y. Lu, J. Zhu, J. Chen, Developments of polyurethane in biomedical applications: a review, Resour. Chem. Mater. 2 (2023) 262.
[18] C.O. Adetunji, O.T. Olaniyan, O.A. Anani, A. Inobeme, J.T. Mathew, Environmental impact of polyurethane chemistry, Polyurethane Chem. Renew. Poly. Isocyanates 393 (2021).
[19] R.V. Gadhave, S. Srivastava, P.A. Mahanwar, P.T. Gadekar, Recycling and disposal methods for polyurethane wastes: a review, Open J. Polym. Chem. 9 (2019) 39.
[20] J. Zeldin, P.P. Chaudhary, J. Spathies, M. Yadav, B.N. D'Souza, M.E. Alishahedani, P. Gough, J. Matriz, A.J. Ghio, Y. Li, Exposure to isocyanates predicts atopic dermatitis prevalence and disrupts therapeutic pathways in commensal bacteria, Sci. Adv. 9 (2023) eade8898.
[21] P. Runwal, 2025, 40 years later, Bhopal is still in crisis. *C&EN*.
[22] J. Guan, Y. Song, Y. Lin, X. Yin, M. Zuo, Y. Zhao, X. Tao, Q. Zheng, Progress in study of non-isocyanate polyurethane, Ind. Eng. Chem. Res. 50 (2011) 6517.
[23] A.K. Ghosh, A. Sarkar, M. Brindisi, The Curtius rearrangement: mechanistic insight and recent applications in natural product syntheses, Org. Biomol. Chem. 16 (2018) 2006.
[24] H. Lebel, O. Leogane, Curtius rearrangement of aromatic carboxylic acids to access protected anilines and aromatic, Ureas Org. Lett. 8 (2006) 5717.
[25] S. Shi, C. Yao, J. Cen, L. Li, G. Liu, J. Hu, S. Liu, High-fidelity end-functionalization of poly (ethylene glycol) using stable and potent carbamate linkages, Angew Chem. Int. Ed. 59 (2020) 18172.
[26] Y. Roeske, W. Abraham, The photochemistry of acyl azides; X: Aroylnitrenes for heterocycle synthesis, Synthesis 112 (2001) 1125.
[27] A. Kocaarslan, G. Yılmaz, G. Topcu, L. Demirel, Y. Yagcı, A novel photoinduced ligation approach for cross-linking polymerization, polymer chain-end functionalization, and surface modification using benzoyl Azides, Macromol. Rapid Commun. 42 (2021) 2100166.
[28] Q. Thijssen, J.A. Carroll, F. Feist, A. Beil, H. Grützmacher, M. Wegener, S. Van Vlierberghe, C. Barner-Kowollik, Beyond absorption maxima: the impact of wavelength-resolved photochemistry on materials science, Mater. Horiz. 11 (2024) 6184.
[29] J.A. Carroll, F. Pashley-Johnson, H. Frisch, C. Barner-Kowollik, Photochemical action plots reveal red-shifted wavelength-dependent photoproduct distributions, Chem Eur J 30 (2024) e202304174.
[30] S.L. Walden, J.A. Carroll, A.N. Unterreiner, C. Barner-Kowollik, Photochemical action plots reveal the fundamental mismatch between absorptivity and photochemical reactivity, Adv. Sci. 11 (2024) 2306014.

[31] I.M. Irshadeen, S.L. Walden, M. Wegener, V.X. Truong, H. Frisch, J.P. Blinco, C. Barner-Kowollik, Action plots in action: in-depth insights into photochemical reactivity, J. Am. Chem. Soc. 143 (2021) 21113.
[32] S.L. Walden, J.A. Carroll, A.N. Unterreiner, C. Barner-Kowollik, Photochemical action plots reveal the fundamental mismatch between absorptivity and photochemical reactivity, Adv. Sci. 11 (2024) 2306014.
[33] C. Wentrup, H. Bornemann, "The Curtius rearrangement of acyl azides revisited–Formation of cyanate (R–O–CN)", Wiley Online Library, 2005.
[34] X.-L. Peng, W.-L. Ding, Q.-S. Li, Z.-S. Li, Theoretical insights into photo-induced Curtius rearrangement of chlorodifluoroacetyl azide, Org. Chem. Front. 4 (2017) 1153.
[35] H.-L. Peng, Why does 4-biphenyl carbonyl azide have ultra-short lived excited states? An ultrafast UV-vis spectroscopic and computational study, Phys. Chem. Chem. Phys. 20 (2018) 29091.
[36] M.E. Sigman, T. Autrey, G.B. Schuster, Aroylnitrenes with singlet ground states: photochemistry of acetyl-substituted aroyl and aryloxycarbonyl azides, J. Am. Chem. Soc. 110 (1988) 4297.
[37] J. Kubicki, Y. Zhang, S. Vyas, G. Burdzinski, H.L. Luk, J. Wang, J. Xue, H.-L. Peng, E.A. Pritchina, M. Sliwa, Photochemistry of 2-Naphthoyl azide. An ultrafast time-resolved UV–Vis and IR spectroscopic and computational study, J. Am. Chem. Soc. 133 (2011) 9751.
[38] R.H. Abu-Eittah, A.A. Mohamed, A.M. Al-Omar, Theoretical investigation of the decomposition of acyl azides: molecular orbital treatment, Int. J. Quantum Chem. 106 (2006) 863.
[39] S. Vyas, J. Kubicki, H.L. Luk, Y. Zhang, N.P. Gritsan, C.M. Hadad, M.S. Platz, An ultrafast time-resolved infrared and UV–vis spectroscopic and computational study of the photochemistry of acyl azides, J. Phys. Org. Chem. 25 (2012) 693.
[40] K.-U. Clauss, K. Buck, W. Abraham, The photochemistry of acyl azides—IX. direct and sensitized photolytic generation of acylnitrenes for cycloaddition reactions, Tetrahedron 51 (1995) 7181.
[41] G.W. Breton, X. Vang, Photodimerization of anthracene, J. Chem. Educ. 75 (1998) 81.
[42] S.P. Pujari, L. Scheres, A.T. Marcelis, H. Zuilhof, Covalent surface modification of oxide surfaces, Angew. Chem. Int. Ed. 53 (2014) 6322.
[43] B. Verbraeken, R. Hoogenboom, Cyclic polymers: from scientific curiosity to advanced materials for gene delivery and surface modification, Angew. Chem. Int. Ed. 56 (2017) 7034.
[44] B. Kiskan, Y. Yagci, Synthesis and characterization of naphthoxazine functional poly (ε-caprolactone), Polymer 46 (2005) 11690.